Molecular Psychiatry
https://doi.org/10.1038/s41380-019-0378-4

ARTICLE

Mechanisms underlying the synaptic trafficking of the glutamate delta receptor GluD1

Wucheng Tao[1] · Chenxue Ma[2] · Michael A. Bemben[1] · Kathy H. Li[3] · Alma L. Burlingame[3] · Mingjie Zhang[2,4] · Roger A. Nicoll[1]

Received: 14 September 2018 / Revised: 29 January 2019 / Accepted: 11 February 2019

Abstract

Ionotropic glutamate delta receptors do not bind glutamate and do not generate ionic current, resulting in difficulty in studying the function and trafficking of these receptors. Here, we utilize chimeric constructs, in which the ligand-binding domain of GluD1 is replaced by that of GluK1, to examine its synaptic trafficking and plasticity. GluD1 trafficked to the synapse, but was incapable of expressing long-term potentiation (LTP). The C-terminal domain (CT) of GluD1 has a classic PDZ-binding motif, which is critical for the synaptic trafficking of other glutamate receptors, but we found that its binding to PSD-95 was very weak, and deleting the PDZ-binding motif failed to alter synaptic trafficking. However, deletion of the entire CT abolished synaptic trafficking, but not surface expression. We found that mutation of threonine (T) T923 to an alanine disrupted synaptic trafficking. Therefore, GluD1 receptors have strikingly different trafficking mechanisms compared with AMPARs. These results highlight the diversity of ionotropic glutamate receptor trafficking rules at a single type of synapse. Since this receptor is genetically associated with schizophrenia, our findings may provide an important clue to understand schizophrenia.

Introduction

Neurons in the central nervous system express three types of ionotropic glutamate receptors: AMPA receptors (AMPARs), NMDA receptors (NMDARs), and kainate receptors (KARs). In addition, there is a fourth type of glutamate receptor that shares high sequence homology with ionotropic receptors referred to as delta receptors (GluD1 and GluD2) [1, 2]. However, these receptors are not gated by glutamate or any known endogenous ligand. GluD2 is specifically expressed in cerebellar Purkinje cells, whereas GluD1 is broadly expressed in the forebrain [3, 4]. Our understanding of GluD receptors comes largely from studies on GluD2. GluD2 is selectively expressed at parallel fiber (PF)-Purkinje cell synapses and genetic deletion results in a 50% loss of PF synaptic transmission and a loss of long-term depression [5, 6]. Recent elegant studies have shown that GluD2 is part of a tripartite transsynaptic scaffold consisting of the soluble glycoprotein cerebellin 1, which binds to GluD2, and presynaptic neurexins [7–9]. This complex is required for both synaptogenesis and synapse maintenance. An analogous role has recently been found for GluD1 at hippocampal excitatory synapses [10]. In contrast to our understanding of the structural role of GluD receptors, little is known about their synaptic trafficking, aside from reports that the C-terminal domain (CT) of GluD2 is important for cerebellar LTD [11–14].

The trafficking of other ionotropic receptors has received considerable attention. Although AMPAR trafficking does not require the CT [15], covalent modifications of the CTs, as well as auxiliary subunits (TARPs) are needed for proper basal and activity-dependent synaptic trafficking [16–19]. The role of CTs in the trafficking of KARs is less clear. While the Neto auxiliary subunits of KARs have dramatic

✉ Roger A. Nicoll
roger.nicoll@ucsf.edu

1 Department of Cellular and Molecular Pharmacology, University of California, San Francisco, CA 94143, USA

2 Division of Life Science, State Key Laboratory of Molecular Neuroscience, Hong Kong University of Science and Technology, Clear Water Bay, Kowloon, Hong Kong, China

3 Department of Pharmaceutical Chemistry, University of California, San Francisco, CA 94158, USA

4 Center of Systems Biology and Human Health, Hong Kong University of Science and Technology, Clear Water Bay, Kowloon, Hong Kong, China

Published online: 01 March 2019

effects on the biophysical properties of these receptors, their role in trafficking is uncertain. A number of studies have found little or limited evidence for a role in trafficking [20–22], while other studies have implicated a trafficking role [19, 23]. NMDARs, for which auxiliary subunits have not been identified, rely primarily on their CTs for synaptic trafficking [24]. Surprisingly, KARs exhibit normal long-term potentiation (LTP) [15] and similar to LTP of AMPAR/TARPs, LTP of GluK/Neto relies on CT domain interactions [19].

Given the extensive knowledge available on the trafficking of ionotropic glutamate receptors, we wished to determine how the mechanisms underlying GluD1 trafficking compared with AMPARs, which share a high degree of homology to GluD1. To track GluD1, we used a pharmacologically tagged version of GluD1 [10]. We found that GluD1 was incapable of expressing LTP. Although the CT of GluD1 has a classic PDZ-binding motif, we found that its binding to PSD-95 was very weak, and deleting the PDZ-binding motif failed to alter synaptic trafficking. However, deletion of the entire CT abolished synaptic trafficking, but not surface expression. We found that mutation of threonine (T) T923 to an alanine disrupted trafficking. Although T923 is a consensus sequence for CaMKII phosphorylation, we were unable to detect phosphorylation of this site with mass spectrometry phosphorylation by CaMKII, PKA, or PKC. Instead, we postulate that mutation of T923 prevents a protein–protein interaction(s) with critical synaptic proteins.

Results

Although the GluD1 receptor is expressed at CA1 synapses, it does not generate current to synaptically released glutamate [10]. Thus to study the trafficking of GluD1, we took advantage of a chimeric receptor, in which the ligand-binding domain (LBD) of the kainate receptor GluK2 replaced the LBD of GluD1 [25, 26]. This receptor, referred to as GluD1-K2, has the pharmacological properties of a kainate receptor and can be distinguished from endogenous AMPARs with the selective AMPAR antagonist GYKI53655 [10]. Since synapses on CA1 pyramidal cells do not express KARs, we used GYKI53655 to study the trafficking of exogenously expressed GluD1 [10]. Our previous studies found that exogenously expressed KARs exhibited normal LTP, indicating that LTP is more promiscuous than previously thought [15]. We therefore wondered if GluD1 receptors might also undergo LTP. We used in utero electroporation to transfect GluD1-K2 into WT mice. Acute slices were prepared from 2-week-old animals, and AMPAR responses were blocked with the AMPAR selective blocker GYKI53655. Neurons expressing GluD1-K2 (green circles) failed to show LTP (Fig. 1a). In fact, there was a highly reproducible depression in the GYKI53655-resistant responses. In a separate set of control experiments with untransfected cells in the absence of GYKI53655 robust, LTP was observed (black circles). To examine this "LTD" in more detail, we repeated the experiments, but instead of expressing GluD1-K2 on a wild-type background, we expressed the construct on an AMPAR-null background. This was accomplished by using mice in which the genes for GluA1-GluA3 were floxed [15, 27, 28], which deletes all functional AMPARs in cells expressing Cre recombinase. We used in utero electroporation to transfect both Cre recombinase and GluD1-K2. Acute slices were prepared from 2-week-old animals, and simultaneous dual whole-cell recordings in the absence of GYKI53655 were made from a transfected cell (with Cre and D1–K2 expression) and a neighboring control cell (the same normal expression of AMPAR as WT). In this case, robust LTP was observed in control cells, but transfected cells failed to show either LTP or LTD (Fig. 1b). Thus, through two different methods, pharmacology (GYKI53655) and genetic deletion of AMPAR subunits, we

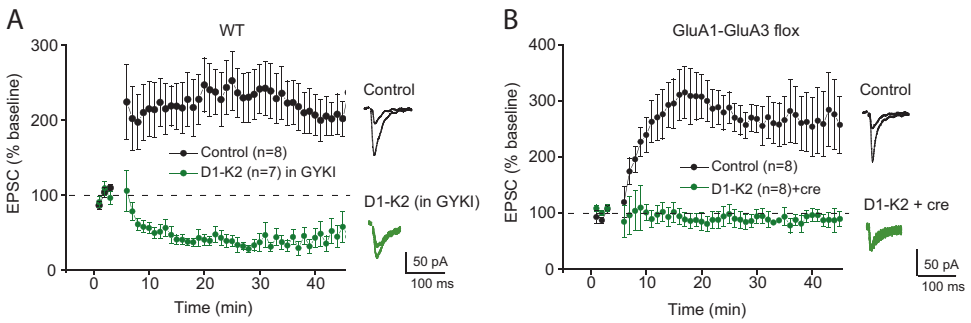

Fig. 1 GluD1 does not express LTP. **a** While control cells in WT mice showed LTP, GluD1-K2 transfected cells (by utero electroporation in WT mice and in the presence of GYKI) showed a pronounced "LTD". **b** We repeated the experiments in (**a**) but used GluA1-GluA3 triple floxed mice. Cells transfected by utero electroporation with GluD1-K2 and cre recombinase did not show either LTP or LTD, while simultaneously recorded control cells showed normal LTP. Black traces are control cells, green are transfected cells. LTP was induced by stimulating at 2 Hz for 90 s while clamping the cell at 0 mV

isolated D1–K2-mediated currents and found that this receptor did not mediated LTP.

Our previous results demonstrated the importance of PDZ domain interactions for both basal transmission and LTP of AMPAR/TARPs and KARs [19]. Given that GluD1 has a classic PDZ-binding motif, the inability of GluD1-K2 to express LTP was surprising. We therefore examined the ability of GluD1 to bind to PSD-95. We used two different assays to test the interaction and compared the binding of GluD1 to that of stargazin (Fig. 2a). Isothermal titration calorimetry (ITC)-based assay using highly purified proteins showed that there is no detectable binding between the entire C-terminal tail (aa 852–1010, GluD1_CT) of GluD1 or the C-terminal PDZ-binding motif (PBM) containing fragment (aa 949–1010; GluD1_PBM) and the full-length PSD-95 (Fig. 2b). In contrast, the entire tail of stargazin (aa 203–323, Stg_CT) was found to bind to PSD-95 with a high affinity (Kd ~ 0.5 μM) (Fig. 2b). We have also adopted a sedimentation-based assay to assess whether there might exist weak interaction between GluD1 and PSD-95 that can lead to liquid–liquid phase separation of the complex [29]. Again, we could not detect any phase separation in the mixtures of GluD1_CT or GluD1_PBM with PSD-95. In contrast, mixtures of Stg_CT with PSD-95 in 1:1 and 1:3 ratios both formed complexes via phase separation (Fig. 2c).

We used either TARP γ-2 or TARP γ-8 in our studies since these TARPs have identical PDZ-binding motifs and behave similarly in our biochemical assays (Zhang, unpublished observations). We next swapped the CT of TARP γ-8 with the CT of GluD1. We refer to this construct as GluD1-K2- γ-8. Perhaps the PDZ-binding motif of TARP γ-8 would permit GluD1 to exhibit LTP. We carried out in utero electroporation in mice and made slices from 2-week-old animals, as described for Fig. 1a. In this case, we observed very little basal synaptic transmission in the presence of GYKI53655 (Fig. 3a). The simultaneously recorded NMDAR responses were of normal size (Fig. 3b). The presence of normal sized NMDAR responses indicates that, although we failed to observe inward currents at negative holding potentials, an adequate number of synapses were activated. In our previous study [10], we found that GluD1 receptors have a synaptogenesis role, and thus enhance

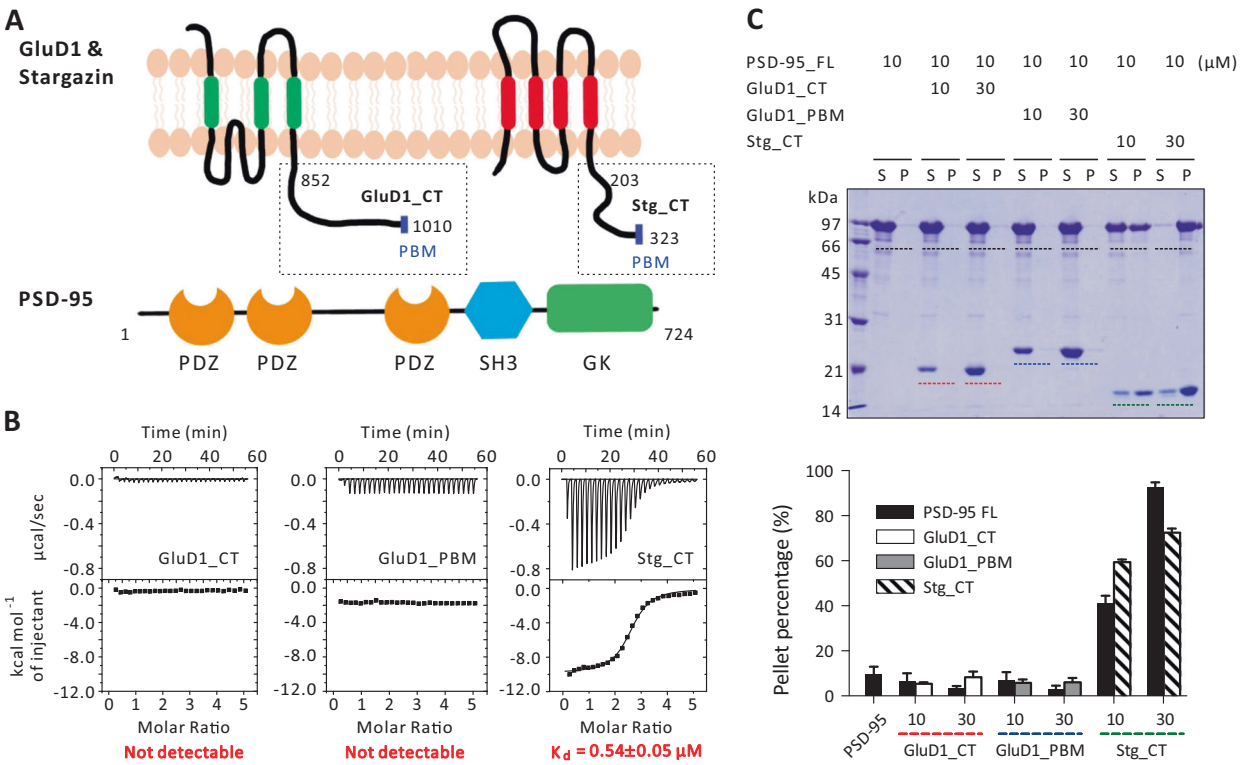

Fig. 2 GluD1 does not bind to PSD-95. **a** Schematic diagram showing the domain organization and topology of GluD1, Stargazin and PSD-95. **b** ITC-based measurement comparing the bindings of GluD1_CT, TRX-GluD1_PBM and Stg_CT to full-length PSD-95. There is no detectable binding between GluD1_CT/GluD1_PBM and PSD-95. As a positive control, Stg_CT robustly binds to PSD-95. In each titration, 250 μM GluD1_CT, TRX-GluD1_PBM or Stg_CT was titrated into full-length PSD-95 at 10 μM. **c** Sedimentation assay showing that neither GluD1_CT nor TRX-GluD1_PBM forms protein complex with full-length PSD-95. Stg_CT interacts with PSD-95 and the complex undergoes phase separation into a condensed phase that can be pelleted by centrifugation [29]. Assay was performed at two different molar ratios (1:1 or 1:3) as indicated. Full-length PSD-95 was kept at 10 μM and GluD1 or Stg was at 10 μM or 30 μM. P represents the protein complex that has been spun down to the pellet. S represents proteins in the supernatant. Quantification data were presented as mean ± SD with results from three independent batches of the sedimentation assay

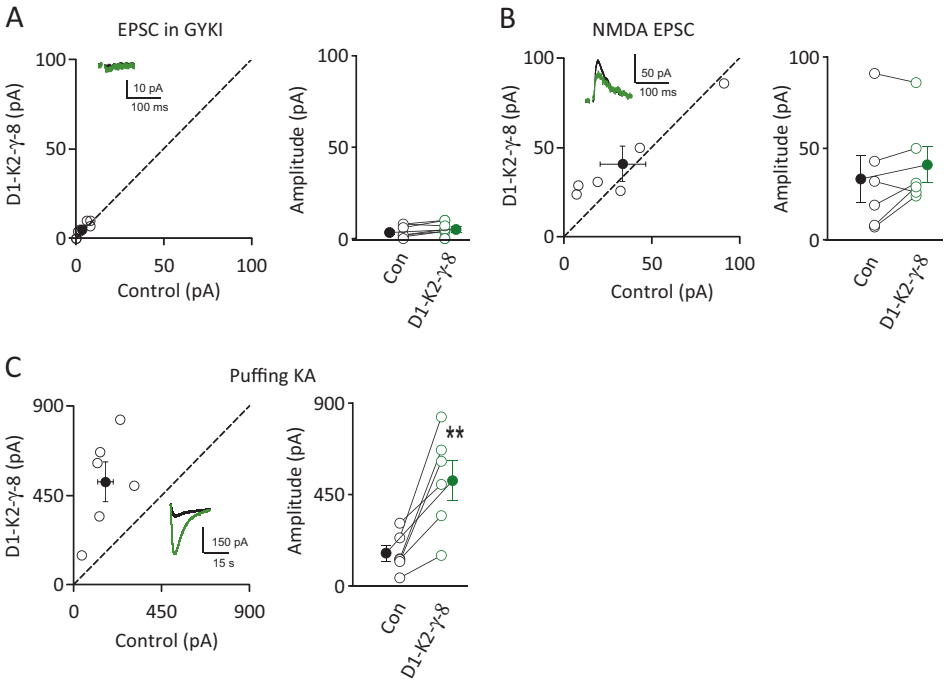

Fig. 3 GluD1-K2-γ-8 does not traffic to hippocampal synapses. **a** In the presence of GYKI, control cells and GluD1-K2-γ-8 transfected cells did not show synaptic inward current (Con: 3.3 ± 1.2 pA; GluD1-K2- γ-8: 5 ± 1.3 pA; $n = 8$, $P > 0.05$). **b** NMDA currents in the group of control cells and GluD1-K2-γ-8 transfected cells are not significantly different (Con: 33.3 ± 12.8 pA; GluD1-K2- γ-8: 41 ± 9.7 pA; $n = 6$, $P > 0.05$). **c** Surface KA currents induced by puffing of KA (1 mM) are larger in the group of GluD1-K2- γ-8 transfected cells (518.5 ± 99.3 pA; $n = 6$) than that of control cells (161.6 ± 39 pA; $n = 6$, $P < 0.01$). Black traces are control cells, green are transfected cells. Open circles are individual pairs, filled circle is mean ± s.e.m. $^{**}P < 0.01$

NMDA EPSCs. Therefore, if GluD1 does not go to the synapse, NMDA EPSCs will not be enhanced, whereas if it goes to the synapse, the NMDA EPSCs will be enhanced. Thus, we use the change of NMDA EPSC as a second readout for GluD1 synaptic targeting. The lack of enhanced NMDAR responses further supports that GluD1-K2-γ-8 is excluded from the synapse [10]. The absence of synaptic responses with GluD1-K2-γ-8 could result from either a lack of expression of a functional receptor on the surface or to an inability of the receptor to traffic to the synapse. We therefore examined the response to the puff application of kainate (KA) and compared the response in control cells to that in simultaneously recorded transfected cells. KA activates both AMPARs and KARs, but has a higher affinity for KARs. Thus, if GluD1-K2-γ-8 is expressed on the surface, the response should be larger in transfected cells. This was, indeed, the case (Fig. 3c). Thus, although this construct is expressed and functional, it is unable to traffic to the synapse.

What might be responsible for the trafficking of GluD1? Perhaps the swap with the TARP γ-8 CT removes a trafficking signal from the GluD1 CT. To address this possibility, we deleted the CT from GluD1. Indeed, this construct (ΔCT) failed to traffic to the synapse (Fig. 4a). To be confident that an adequate number of synapses had been activated in these experiments, we carried out a stimulus–response curve (Fig. 4b) and found that the response saturated at 100 µA. Thus for these experiments, we routinely used stimuli greater than 100 µA. To determine if the ΔCT construct was expressed on the surface, we compared the response to puffing KA in control cells to that recorded in transfected cells. Cells expressing the ΔCT construct responded more strongly to the application of kainate than control cells (Fig. 4c). Thus, although this CT truncated receptor still gets to the surface and is functional, it is unable to target to the synapse. We made a series of deletions and narrowed the critical region in the CT. Deletion of the PDZ-binding motif (ΔPDZ) or the distal half of the CT (Δdistal half) had no effect on the responses. However, deletion of the proximal half (Δprox half) or just the last 10 amino acids in the proximal half (Δaa) (Fig. 4d) abolished responses (Fig. 4d).). To further narrow down the key residue, a point mutation at T923 in this 10 amino acid region was made, based on residue conservation in the delta receptor family and potential phosphorylation sites (NetPhos 3.1 server), and we found that T923 was critical for trafficking. Thus replacing this threonine with an alanine, prevented the synaptic targeting of GluD1 (Figs. 4a, 5a, b). Responses to puffed KA demonstrated that this mutation did not affect GluD1 surface trafficking (Fig. 5c). In support of this conclusion, immunostaining of GluD1 confirmed that this mutation prevented GluD1 targeting to synapses (Fig. 5d). Interestingly, when we mutated this single residue of GluD1-K2 to an aspartate (T923D), it had the same phenotypes as wt GluD1, targeting to the synapse and enhancing NMDAR responses (Fig. 6a, b).

These results raise the possibility that T923 might be a target for phosphorylation. Indeed, this site is predicted to be a substrate for CaMKII (NetPhos 3.1). We therefore tested this possibility directly using mass spectroscopy. An

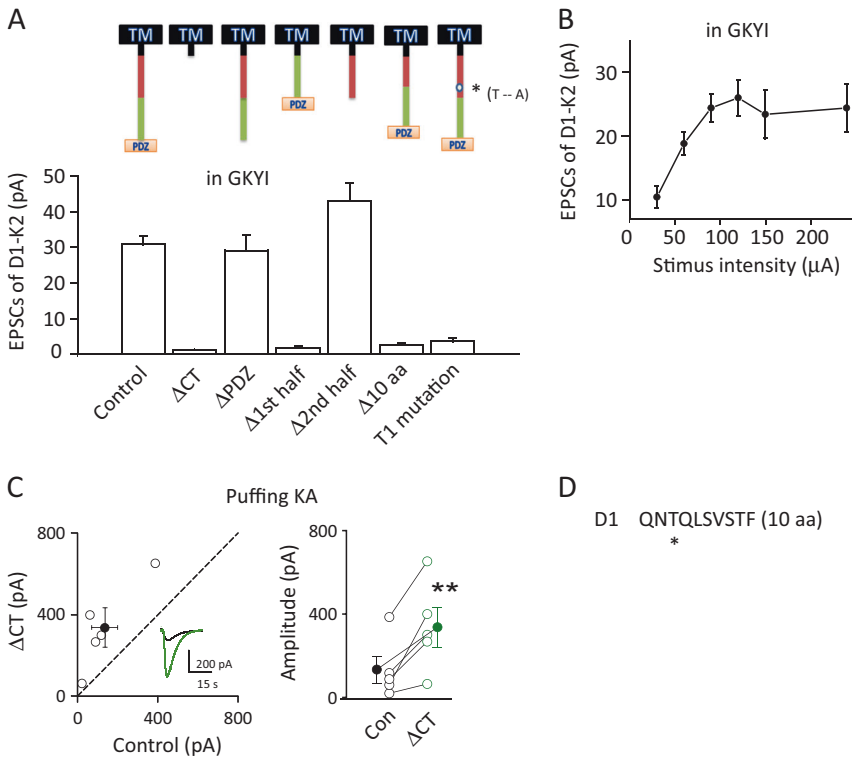

Fig. 4 A single amino acid residue (T923) at the C-terminal domain of GluD1 is required for its synaptic targeting. **a** Basic characteristics of GluD1 with deletions of different segment of CT and their synaptic current responses. **b** Current–stimulus intensity curve of GluD1-K2 ($n = 5$). **c** Surface KA currents induced by puffing of KA (1 mM) are larger in the group of GluD1-CT transfected cells (337.4 ± 95.8 pA; $n = 5$) than that of control cells (134.2 ± 64.9 pA; $n = 5$, $P < 0.01$). Black traces are control cells, green are transfected cells. Open circles are individual pairs, filled circle is mean ± s.e.m. $^{**}P < 0.01$. **d** Sequence of amino acids containing T923 that affects GluD1 synaptic targeting

in vitro kinase assay with engineered glutathione S-transferase (GST) fusion proteins containing the CT of GluD1 and GluA1 was performed as described in ref. [30]. However, constitutively active CaMKII failed to phosphorylate this site (Fig. 6d, e), although it robustly phosphorylated GluA1 at S831, an established target for CaMKII [31, 32]. Furthermore, we were unable to detect phosphorylation of T923 by constitutively active PKC, although it did phosphorylate GluA1 at S831 [33]. Finally, constitutively active PKA failed to phosphorylate T923, although it did phosphorylate GluA1 at S845 [33] (Fig. 6c–e). Thus, in this study, T923 is not phosphorylated by PKC, PKA, or CaMKII. It is possible that an unidentified kinase is involved. It is also possible that T923 undergoes some other protein modifications instead of phosphorylation. In sum, these negative findings suggest that T923 is involved in protein–protein interactions that are necessary for synaptic targeting of GluD1.

Discussion

Although glutamate delta receptors were cloned more than two decades ago, until recently their roles in the CNS remained enigmatic. In cerebellar Purkinje cells, GluD2 is selectively expressed at PF synapses where it binds to the soluble glycoprotein cerebellin 1, which also binds to the presynaptic neurexin. This tripartite transsynaptic complex plays a critical role in synaptogenesis and synapse maintenance [7–9]. A similar role has recently been reported for GluD1 at hippocampal CA1 excitatory synapses [10]. However, little is known concerning the mechanisms underlying the synaptic trafficking of GluD receptors. We find that the trafficking properties of GluD1 are fundamentally different from that of AMPARs. In contrast to AMPAR/TARPs, GluD1 receptor trafficking does not rely on PDZ domain interactions and fails to express LTP. Furthermore, unlike AMPARs, GluD1 trafficking requires the presence of its CT. More specifically, the mutation of T923 to alanine disrupts the synaptic targeting of GluD1. Although T923 is not phosphorylated by PKC, PKA, or CaMKII, it is possible that an unidentified kinase is involved. Alternatively, this mutation might abrogate the binding of GluD1 to critical synaptic proteins. Our findings indicate that, although GluD1 and AMPARs share considerable sequence homologue, the mechanisms underlying their synaptic trafficking are strikingly different.

To study the trafficking of GluD1, we utilized a chimeric construct in which the LBD of GluD1 was replaced with that of GluK2 [2, 25, 26], referred to as GluD1-K2. With this chimeric receptor, we were able to track synaptic trafficking with electrophysiological recording. We previously showed that KARs express normal LTP, indicating that LTP is more promiscuous than generally thought [15, 19]. However, wild-type neurons expressing GluD1-K2 failed to show LTP. Surprisingly, they exhibited a strong LTD. We

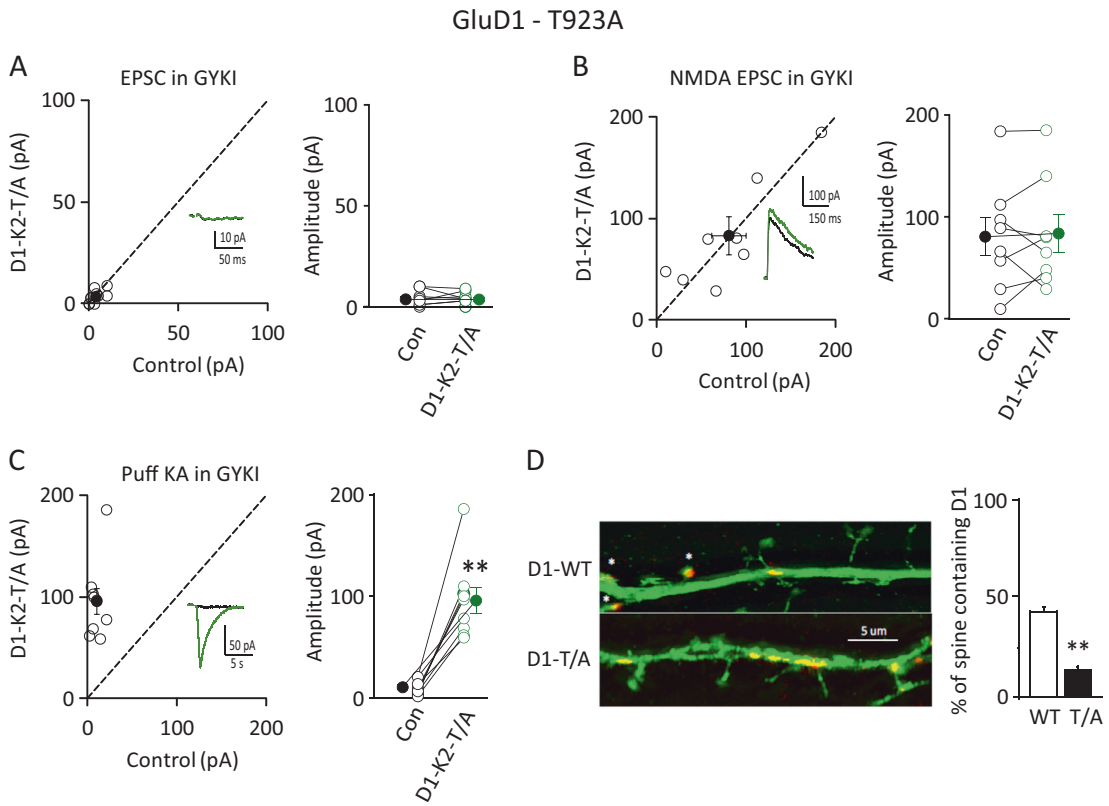

Fig. 5 T923 does not affect surface current of GluD1. **a** GluD1 with T923A mutation did not show synaptic current (Con: 3.7 ± 1.1 pA; T923A: 3.6 ± 1.0 pA; $n = 10$, $P > 0.05$). **b** NMDA currents were not significantly different between control cells (80.4 ± 19.1 pA) and GluD1 T923A expressing cells (83.5 ± 18.8 pA; $n = 8$, $P > 0.05$). **c** In the presence of GYKI, surface current generated by puffing of KA in control cells and GluD1 T923A cells (Con: 10.1 ± 2.3 pA; T923A: 96 ± 12.8 pA; $n = 9$, $P < 0.01$). Black traces are control, green are experimentally transfected. Open circles are individual pairs, filled circle is mean ± s.e.m. **d** Immunostaining of spine and GluD1 showing that T923A significantly reduced GluD1 targeting to synapses. (Con: 43.2 ± 2%; T923A: 13.6 ± 1%; $n = 15$, $P < 0.01$). $^{**}P < 0.01$

repeated these experiments, but on an AMPAR-null background by coexpressing Cre in triple-floxed mice [15] together with GluD1-K2. In this case, LTP induction resulted in no change in the GluD1-K2 responses. What might account for the difference in these two results? One possibility is that GluD1-K2 can occupy AMPAR slots, but is incapable of expressing LTP. In wild-type cells, the LTP induced trafficking of AMPARs displaces GluD1-K2 from the slots, thus resulting in an LTD. The notion is that constitutively trafficked GluD1-K2 can occupy the same slots that AMPARs occupy. When LTP is induced, GluD1-K2 is unable to express LTP, whereas AMPARs are recruited to the synapse and displace GluD1-K2 from some of the slots. This recruitment of AMPARs is "silent" because GYKI53655 blocks their activation. In the absence of competing AMPARs, the induction of LTP has no effect on GluD1-K2 responses, supporting this scenario.

Why does GluD1-K2 fail to undergo LTP? Previous results found that PDZ domain interactions are required for the expression of LTP mediated either by AMPAR/TARPs or by GluK1/Neto [19]. The CT of the GluD1 receptor has a classic PDZ-binding motif, and therefore it was a surprise that it failed to express LTP. However, based on two different binding assays, we found that, compared with the robust binding of the CT of stargazin to the scaffolding protein PSD-95, the binding of the CT of GluD1 to PSD-95 was very weak. How might this result be reconciled with a previous study reporting an interaction between GluD2 with PSD-93 [34]? In this study, a yeast two-hybrid-based assay showed that GluD1/2 could bind to PDZ domains of PSD-93/95 connected in the tandem, but the binding between GluD1/2 with individual PDZ domains of PSD-95 was not detectable or very weak. It is possible that the Gal4 DNA-binding domain-mediated dimerization of the GluD1/2 tail in the yeast two-hybrid screening enhanced the avidity of the very weak binding between GluD1/2 and PSD-93/95.

In an attempt to confer LTP onto GluD1, we swapped the CT of GluD1 with that of CT of TARP γ-8 (GluD1-K2- γ-8), which binds strongly to PSD-95. However, this construct failed to traffic to the synapse, even under basal conditions, although it was expressed on the surface, albeit in low amounts. The inability of the GluD1-K2-γ-8 to target to synapses raises the possibility that the CT of GluD1-K2 is necessary for synaptic localization. Indeed, deleting the CT of

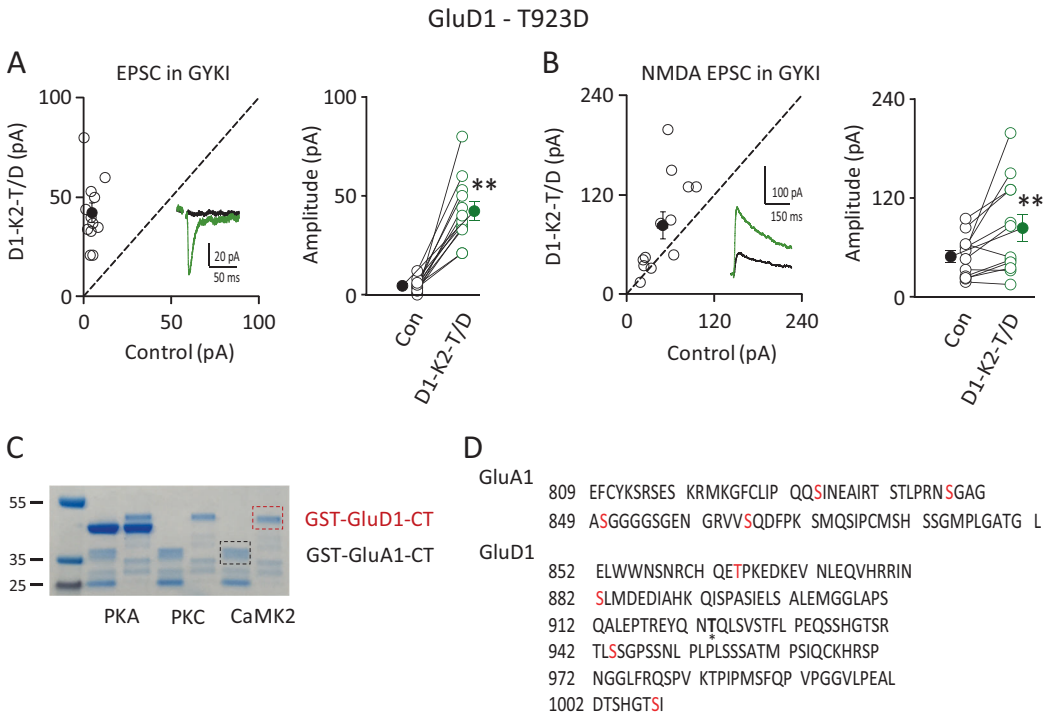

E

Residue(GluA1)	Sequence	Kinase
S845*	NSGAGASGGGGSGENGR	PKA
S850	NSGAGASGGGGSGENGRVVSQDFPK	PKA
S863	VVSQDFPK	PKA
S831*	MKGFCLIPQQSINEAIR	PKC, CaMK2

Residue(GluD1)	Sequence	Kinase
T864	CHQETPKEDKEVNLEQVHR	PKA, PKC
S882	RINSLMDEDIAHK	PKA, CaMK2
S944	TLSSGPSSNLPLPLSSSATMPSIQCK	PKA
S1008	TPIPMSFQPVPGGVLPEALDTSHGTSI	PKA

Fig. 6 Phosphorylation of GluD1 T923. **a** T923D had the same phenotype as wt GluD1 generating GYKI-resistant currents (Con: 4.54 ± 0.9 pA; T923D: 42.3 ± 4.8 pA; $n = 12$, $P < 0.01$). **b** Similar to wt GluD1, T923D increased NMDA currents (Con: 48.9 ± 7.3 pA; T923D: 83.5 ± 16.5 pA; $n = 12$, $P < 0.01$); Black traces are control cells, green are transfected cells. Open circles are individual pairs, filled circle is mean ± s.e.m. **c** Coomassie staining of GST-GluA1 and GST-GluD1. **d** Sequence of CT of GluA1 and GluD1. **e** MS analysis for phosphorylation of CTD of GluA1 and GluD1 by PKA, PKC, and CaMKII. $^{**}P < 0.01$. Note, phosphorylation residues are highlighted in red. Phosphorylation of S845* and S831* have been reported in previous publications

GluD1-K2 prevented its synaptic targeting, even though the receptor was delivered to the surface. Further experiments established that the mutation of T923 to an alanine disrupted synaptic delivery, whereas GluD1 with threonine mutated to an aspartate behaved like wt GluD1. Might T923 be a target for phosphorylation? We used mass spectrometry to directly examine whether CaMKII, PKA, or PKC were able to phosphorylate this amino acid. None of these kinases phosphorylated T923, although our experiments leave open the possibility that other unidentified kinases are involve. If T923 is phosphorylated, the finding that the phosphomimic construct (T923D) behaves like wt GluD1, would imply that this

site must be constitutively phosphorylated. Alternatively, if T923 is not phosphorylated, the results suggest that T923 may be critical in binding of GluD1 to an as yet unidentified synaptic protein.

Conclusion

GluD1 receptors play a critical role in synaptogenesis and synapse maintenance in the hippocampus. The present study analyzed the properties underlying the synaptic trafficking of GluD1 at CA1 hippocampal synapses and how this trafficking compares to AMPARs. We find that GluD1 receptors have strikingly different trafficking mechanisms compared with AMPARs. Whereas the trafficking of AMPAR/TARPs relies on PDZ domains interactions, GluD1 does not. While AMPARs can traffic to the synapse in the absence of their CT, relying instead on auxiliary TARPs, GluD1 does require an intact CT. Finally, GluD1 receptors failed to exhibit LTP. These results highlight the diversity of ionotropic glutamate receptor trafficking rules at a single type of synapse.

Methods

Animals

GluA1-A3 Triple flox mice were generated as previously described [27]. All experimental procedures on animals were approved by the UCSF Animal Care and Use Committee.

Experimental constructs

The GluD1 and GluD1-K2 plasmids were obtained from Dr. Michael Hollmann. For biolistic experiments, all plasmids were expressed in pCAGGS vector, which contains an internal ribosome entry site (IRES) followed by the fluorophore GFP. All the deletions and mutations were obtained by overlapping PCR method followed by In-Fusion cloning (Clontech).

Slice culture and biolistic transfection

Hippocampal cultured slices were obtained from 6- to 8-day-old rats or mice [35]. Biolistic transfection was done 1 day after sectioning, by using a Helio Gene Gun with 1 µm of DNA-coated gold particles (Bio-Rad). Slices were maintained at 34 °C, and the medium was changed every 2 days.

Acute slice preparation

Mice aged of 2–3 weeks were anesthetized with 4% isoflurane, decapitated, and the brain dissected free. The whole brain was sliced into 300 µm slices in cutting solution as described [15]; recovery at 34 °C for half an hour and then stored at room temperature. Solutions were continuously gassed with 95% O_2/5% CO_2.

Electrophysiological recording

Dual whole-cell voltage clamp recordings were obtained from a fluorescent transfected cell and a neighboring control pyramidal cell in the CA1 region of the hippocampus [36]. Pyramidal neurons were identified by location and morphology. All recordings were made at 20–25 °C. Internal solution (in mM): 135 $CsMeSO_4$, 8 NaCl, 10 HEPES, 5 QX314-Cl, 4 Mg-ATP, 0.3 Na-GTP, 0.3 EGTA, and 0.1 spermine. Osmolarity was adjusted to 290–295 mOm, and pH was buffered at 7.3–7.4. External solution (mM): 119 NaCl, 2.5 KCl, 4 $CaCl_2$, 4 $MgCl_2$, 1 NaH_2PO_4, 26.2 $NaHCO_3$, 11 glucose, bubbled continuously with 95% O_2/5% CO_2. Synaptic currents were evoked by bipolar electrode stimulation of Schaffer collaterals. To record EPSCs, picrotoxin (100 µM) was added into external solution; for recording AMPA EPSCs, the cell was held at −70 mV, while for NMDA EPSCs, it was held at + 40 mV and the NMDA component was measured 100 ms after the stimulus; LTP was induced by stimulating at 2 Hz for 90 s while clamping the cell at 0 mV. Current responses were collected with a Multiclamp 700B amplifier (Axon Instruments), filtered at 2 kHz, and digitized at 10 kHz. Cells with series resistance larger than 20 MOhm were excluded from analysis.

Imaging

Slice cultures were biolistically transfected with GFP or other DNA constructs. One week later, slices were fixed with 4% paraformaldehyde/sucrose in PBS, permeabilized with 0.1% TritonX-100, and stained with anti-GFP antibody (Invitrogen), followed by a goat antibody to rabbit conjugated to Alexa Fluor 488 (Invitrogen). Slices were mounted with Flouromount-G (South Biotech) and stored at 4 °C until use. For spine measurements, images were acquired with a 100x oil object under super-resolution microscopy (N-SIM Microscope System, Nikon) and analyzed with supplied software (NIS-Elements, Nikon). Neurons were imaged for a length of 100 µm of primary apical dendrites, starting 100 µm from the cell body.

Protein expression and purification

Various recombinant proteins were expressed with the N-terminal TRX-His6-affinity tag in *E. coli* BL21 cells. Nickel–NTA affinity column and size-exclusion chromatography (Superdex 200 or Superdex 75) were used for the

first round of protein purification with a buffer containing 100 or 300 mM NaCl, 50 mM Tris, pH 8.2, 2 mM DTT, and 1 mM EDTA. For the PSD-95 full-length protein (Uniprot: P78352, aa 1–724), a mono Q column was used to separate the protein degradation contamination. Untagged GluD1_CT (Uniprot: Q61627, aa 852–1010) and TRX-tagged GluD1_PBM (aa 949–1010) could be purified with high qualities by another step of gel filtration column using Superdex 75. After tag cleavage, a mono S column was used to separate the TRX tag and DNA contaminations from Stargazin_CT (Uniprot: O88602, aa 203–323). Finally, highly purified proteins were exchanged into the assay buffer containing 100 mM NaCl, 50 mM Tris, pH 8.2, 2 mM DTT, and 1 mM EDTA by a desalting column.

Isothermal titration calorimetry (ITC) assay

Proteins used for ITC assay were prepared in buffer containing 100 mM NaCl, 50 mM Tris, pH 8.2, 2 mM DTT, and 1 mM EDTA. Assay was performed at 25 °C on a Microcal VP-ITC calorimeter. Protein concentrations for each titration are indicated in the figure legend. Titration data were analyzed and fitted by Origin 7.0 software.

Sedimentation assay detecting protein complex formation

All protein samples were in the buffer containing 100 mM NaCl, 50 mM Tris, pH 8.2, 2 mM DTT, and 1 mM EDTA. The final volume of each reaction sample was 100 µl. After mixing different protein components at the indicated concentrations, protein mixtures were incubated at room temperature for 10 min and then centrifuged at 14,000 *g* for 10 min at 22 °C in a bench-top centrifuge. After centrifugation, supernatants were immediately transferred to a new tube and pellets were thoroughly resuspended by 100 µl of buffer. Equal volumes of SDS loading dye were added to both supernatant and resuspended pellet solutions and protein distributions were analyzed by 10% SDS-PAGE. Band intensities were quantified by the ImageJ software.

Phosphorylation assay

GST fusion proteins were obtained from BL21 bacterial cells transformed with pGEX-GluA1 and pGEX-GluD1 as described [30]. PKA, PKC, and CaMKII in vitro phosphorylation assays were described in ref. [30]. The kinase assays were performed at 30 °C for 30 min and were discontinued by adding SDS-PAGE sample buffer and boiled 95 °C for 5 min. The proteins were resolved by SDS-PAGE and then were stained with Coomassie blue. The samples in Coomassie staining gel were cut out and were resolved by mass spectrometry (UCSF, Biomedical Mass Spectrometry and Proteomics Resource Center).

Protein identification using reversed-phase liquid chromatpgraphy electrospry tendem mass spectrometry (LC-MS/MS)

The targeted gel bands were excised from a gel and subjected to tryptic digestion. The peptides formed from the digested samples were analyzed by on-line LC-MS/MS technique. The LC separation was carried out on a NanoAcquity UPLC system (Waters), and the MS/MS analysis was performed using Q Exactive Plus Orbitrap mass spectrometer (Thermo Scientific). The acquired MS/MS data from mass spectrometry were searched against UniProt database and the protein sequences of interest with an in-house search engine Protein Prospector (http://prospector.ucsf.edu/prospector/mshome.htm).

Statistical analysis

All paired recording data were analyzed statistically with a Wilcoxon signed-rank test for paired data. For unpaired data, a Wilcoxon–Mann–Whitney rank sum test was used. Statistical comparisons between sets of paired data were done using the Mann–Whitney U test. All statistical tests performed were two sided, and with all tests a p-value of < 0.05 was considered statistically significant. All error bars represent standard error of the mean.

Acknowledgements We thank Dr. Michael Hollmann for the GluD1 and GluD1-K2 plasmids and Dr. Menglong Zeng for helping with the experiments on the GluD1/PSD-95 binding assay. We thank members of the Nicoll lab for comments on the paper. We appreciate the technical assistance from Dan Qin. This research was supported by grants from NIMH and RGC of Hong Kong.

Compliance with ethical standards

Conflict of interest The authors declare that they have no conflict of interest.

References

1. Traynelis SF, Wollmuth LP, McBain CJ, Menniti FS, Vance KM, Ogden KK, et al. Glutamate receptor ion channels: structure, regulation, and function. Pharmacol Rev. 2010;62:405–96.
2. Schmid SM, Hollmann M. Bridging the synaptic cleft: lessons from orphan glutamate receptors. Sci Signal. 2010;3:pe28.
3. Konno K, Matsuda K, Nakamoto C, Uchigashima M, Miyazaki T, Yamasaki M, et al. Enriched expression of GluD1 in higher brain

regions and its involvement in parallel fiber-interneuron synapse formation in the cerebellum. J Neurosci. 2014;34:7412–24.
4. Hepp R, Hay YA, Aguado C, Lujan R, Dauphinot L, Potier MC, et al. Glutamate receptors of the delta family are widely expressed in the adult brain. Brain Struct Funct. 2015;220:2797–815.
5. Kashiwabuchi N, Ikeda K, Araki K, Hirano T, Shibuki K, Takayama C, et al. Impairment of motor coordination, Purkinje cell synapse formation, and cerebellar long-term depression in GluR delta 2 mutant mice. Cell. 1995;81:245–52.
6. Hirai H, Launey T, Mikawa S, Torashima T, Yanagihara D, Kasaura T, et al. New role of delta2-glutamate receptors in AMPA receptor trafficking and cerebellar function. Nat Neurosci. 2003;6:869–76.
7. Uemura T, Lee SJ, Yasumura M, Takeuchi T, Yoshida T, Ra M, et al. Trans-synaptic interaction of GluRdelta2 and Neurexin through Cbln1 mediates synapse formation in the cerebellum. Cell. 2010;141:1068–79.
8. Matsuda K, Miura E, Miyazaki T, Kakegawa W, Emi K, Narumi S, et al. Cbln1 is a ligand for an orphan glutamate receptordelta2, a bidirectional synapse organizer. Science. 2010;328:363–8.
9. Matsuda K, Yuzaki M. Cbln family proteins promote synapse formation by regulating distinct neurexin signaling pathways in various brain regions. Eur J Neurosci. 2011;33:1447–61.
10. Tao W, Diaz-Alonso J, Sheng N, Nicoll RA. Postsynaptic delta1 glutamate receptor assembles and maintains hippocampal synapses via Cbln2 and neurexin. Proc Natl Acad Sci USA. 2018;115:E5373–E5381.
11. Kohda K, Kakegawa W, Matsuda S, Nakagami R, Kakiya N, Yuzaki M. The extreme C-terminus of GluRdelta2 is essential for induction of long-term depression in cerebellar slices. Eur J Neurosci. 2007;25:1357–62.
12. Matsuda S, Hannen R, Matsuda K, Yamada N, Tubbs T, Yuzaki M. The C-terminal juxtamembrane region of the delta 2 glutamate receptor controls its export from the endoplasmic reticulum. Eur J Neurosci. 2004;19:1683–90.
13. Nakagami R, Kohda K, Kakegawa W, Kondo T, Kato N, Yuzaki M. Phosphorylation of delta2 glutamate receptors at serine 945 is not required for cerebellar long-term depression. Keio J Med. 2008;57:105–10.
14. Yawata S, Tsuchida H, Kengaku M, Hirano T. Membrane-proximal region of glutamate receptor delta2 subunit is critical for long-term depression and interaction with protein interacting with C kinase 1 in a cerebellar Purkinje neuron. J Neurosci. 2006;26:3626–33.
15. Granger AJ, Shi Y, Lu W, Cerpas M, Nicoll RA. LTP requires a reserve pool of glutamate receptors independent of subunit type. Nature. 2013;493:495–500.
16. Malinow R, Malenka RC. AMPA receptor trafficking and synaptic plasticity. Annu Rev Neurosci. 2002;25:103–26.
17. Huganir RL, Nicoll RA. AMPARs and synaptic plasticity: the last 25 years. Neuron. 2013;80:704–17.
18. Collingridge GL, Peineau S, Howland JG, Wang YT. Long-term depression in the CNS. Nat Rev Neurosci. 2010;11:459–73.
19. Sheng N, Bemben MA, Diaz-Alonso J, Tao W, Shi YS, Nicoll RA. LTP requires postsynaptic PDZ-domain interactions with glutamate receptor/auxiliary protein complexes. Proc Natl Acad Sci USA. 2018;115:3948–53.
20. Copits BA, Swanson GT. Dancing partners at the synapse: auxiliary subunits that shape kainate receptor function. Nat Rev Neurosci. 2012;13:675–86.
21. Straub C, Tomita S. The regulation of glutamate receptor trafficking and function by TARPs and other transmembrane auxiliary subunits. Curr Opin Neurobiol. 2012;22:488–95.
22. Zhang W, St-Gelais F, Grabner CP, Trinidad JC, Sumioka A, Morimoto-Tomita M, et al. A transmembrane accessory subunit that modulates kainate-type glutamate receptors. Neuron. 2009;61:385–96.
23. Sheng N, Shi YS, Lomash RM, Roche KW, Nicoll RA. Neto auxiliary proteins control both the trafficking and biophysical properties of the kainate receptor GluK1. Elife. 2015;4:e11682.
24. Sanz-Clemente A, Nicoll RA, Roche KW. Diversity in NMDA receptor composition: many regulators, many consequences. Neuroscientist. 2013;19:62–75.
25. Schmid SM, Kott S, Sager C, Huelsken T, Hollmann M. The glutamate receptor subunit delta2 is capable of gating its intrinsic ion channel as revealed by ligand binding domain transplantation. Proc Natl Acad Sci USA. 2009;106:10320–5.
26. Orth A, Tapken D, Hollmann M. The delta subfamily of glutamate receptors: characterization of receptor chimeras and mutants. Eur J Neurosci. 2013;37:1620–30.
27. Lu W, Shi Y, Jackson AC, Bjorgan K, During MJ, Sprengel R, et al. Subunit composition of synaptic AMPA receptors revealed by a single-cell genetic approach. Neuron. 2009;62:254–68.
28. Diaz-Alonso J, Sun YJ, Granger AJ, Levy JM, Blankenship SM, Nicoll RA. Subunit-specific role for the amino-terminal domain of AMPA receptors in synaptic targeting. Proc Natl Acad Sci USA. 2017;114:7136–41.
29. Zeng M, Chen X, Guan D, Xu J, Wu H, Tong P, et al. Reconstituted postsynaptic density as a molecular platform for understanding synapse formation and plasticity. Cell. 2018;174:1172–87 e1116.
30. Bemben MA, Shipman SL, Hirai T, Herring BE, Li Y, Badger JD 2nd, et al. CaMKII phosphorylation of neuroligin-1 regulates excitatory synapses. Nat Neurosci. 2014;17:56–64.
31. Barria A, Muller D, Derkach V, Griffith LC, Soderling TR. Regulatory phosphorylation of AMPA-type glutamate receptors by CaM-KII during long-term potentiation. Science. 1997;276:2042–5.
32. Mammen AL, Kameyama K, Roche KW, Huganir RL. Phosphorylation of the alpha-amino-3-hydroxy-5-methylisoxazole4-propionic acid receptor GluR1 subunit by calcium/calmodulin-dependent kinase II. J Biol Chem. 1997;272:32528–33.
33. Roche KW, O'Brien RJ, Mammen AL, Bernhardt J, Huganir RL. Characterization of multiple phosphorylation sites on the AMPA receptor GluR1 subunit. Neuron. 1996;16:1179–88.
34. Roche KW, Ly CD, Petralia RS, Wang YX, McGee AW, Bredt DS, et al. Postsynaptic density-93 interacts with the delta2 glutamate receptor subunit at parallel fiber synapses. J Neurosci. 1999;19:3926–34.
35. Stoppini L, Buchs PA, Muller D. A simple method for organotypic cultures of nervous tissue. J Neurosci Methods. 1991;37:173–82.
36. Schnell E, Sizemore M, Karimzadegan S, Chen L, Bredt DS, Nicoll RA. Direct interactions between PSD-95 and stargazin control synaptic AMPA receptor number. Proc Natl Acad Sci USA. 2002;99:13902–7.